2023 IEEE International Conference on Robotics and Automation (ICRA 2023)
May 29 - June 2, 2023. London, UK

A Model-Based Analysis of The Effect of Repeated Unilateral Low Stiffness Perturbations on Human Gait: Toward Robot-Assisted Rehabilitation

Vaughn Chambers and Panagiotis Artemiadis*, *IEEE Senior Member*

***Abstract*— Human gait is quite complex, especially when considering the irregular and uncertain environments that humans are able to walk in. While unperturbed gait in a controlled environment is understood to a large degree, gait in more unique environments, such as asymmetric compliant terrain, is not understood to the same degree. In this study, we build upon a neuromuscular gait model and extend it to allow for walking on unilaterally compliant (soft) surfaces. This model is then compared to and verified by experimental human data. The model can successfully walk with step length trends similar to human data. Additionally, the model shows similar behaviors with respect to kinematics and muscle activity. We believe this work contributes significantly to a better understanding of the control of human gait and could lead to model-informed, patient-specific rehabilitation strategies that can advance the field of rehabilitation robotics, as well as the development of bio-inspired controllers for bipedal robots that would be able to traverse through dynamic and complaint terrains.**

I. Introduction

Locomotion is nearly vital for human life, and the most common mode of human locomotion is walking. The average American takes about 5000 steps per day, equaling around 2.5 miles, but studies have shown individuals with active jobs walk much more [1, 2]. As walking plays both an important and frequent role in human life, understanding and modeling the control of gait is of high importance. Gait in a controlled environment with level, rigid ground, and no external perturbations is alone quite complicated and does not accurately simulate all the difficulties of traversing in the real world. In order to develop effective rehabilitation strategies for paretic gait and controllers for more capable bipedal robots, we must seek to understand and model the control of gait in a variety of environments.

Although the control of human gait is understood to a degree, most of our knowledge on gait makes the assumption of a rigid walking surface. While gait on compliant surfaces has indeed been investigated, it has not been examined to the same degree [3–5]. More specifically, understanding and modeling the human response to unilateral low-stiffness environments can offer a unique window into the understanding of the control of human gait. This is due to these environments directly affecting inter-leg coordination, a process of utmost importance in human gait [6]. Moreover, it has been recently shown that walking in unilateral low-stiffness environments evokes responses to the contralateral leg that are mediated through supraspinal pathways [7–9]. While one-step unilateral low stiffness perturbations have been adequately described by a previous model [10], steady state gait in unilaterally compliant environments has not yet been modeled to the level of accuracy needed to explain human gait in those environments.

We believe that understanding and modeling gait in this unusual environment could lead to advances in two main application areas: rehabilitation of paretic gait and development of controllers for bipedal robots. As pertains to rehabilitation, interlimb coordination plays an important role in post-stroke gait as patients are often left with hemiparesis, the weakening of one side of the body [11, 12]. The asymmetric physical difficulties from stroke frequently make it difficult for the legs to properly work together and keep an individual balanced and upright. The ability to accurately model human gait on unilaterally soft terrain would be extremely beneficial to rehabilitation in this area, possibly allowing for patient-specific rehabilitation and treatment. This is supported by our recent work, which revealed that repeated unilateral stiffness perturbations lead to lasting aftereffects once the perturbations have ceased [13]. The main functional aftereffect shown in our study, overall step length increase, is supported by muscle activity data and appears to be quite useful for stroke rehabilitation.

Additionally, the development and control of bipedal robots would greatly benefit from a proper understanding and the capability to accurately model gait on unilaterally soft surfaces. As the goal for bipedal robots is to be robust enough to travel across all terrains, understanding and modeling gait in this unique circumstance is valuable. Currently, bipedal robots are being equipped to detect different terrains and their stiffness values with onboard sensors [14–16]. While slow gait across moderate stiffness terrains is possible, significant progress still needs to be made to allow for smooth and efficient gait across soft terrains [17]. Furthermore, to the best of our knowledge, unilaterally soft environments have yet to be explored in bipeds. Having a comprehensive three-dimensional gait model capable of accurately simulating walking on this terrain would be greatly beneficial for this field of work.

In this paper, we build upon an existing neuromuscular gait model [18] and expand its functionality to describe walking in a unilaterally soft environment. The resulting model was validated by comparing its generated functional, kinematic, and muscle activity data to real experimental

*This material is based upon work supported by the National Science Foundation under Grants No. #2020009, #2015786, #2025797, and #2018905, and the National Institute of Health Grant No. 1R01HD111071-01

Vaughn Chambers and Panagiotis Artemiadis are with the Mechanical Engineering Department, at the University of Delaware, Newark, DE 19716, USA. vaughn@udel.edu, partem@udel.edu

*Corrresponding author: partem@udel.edu

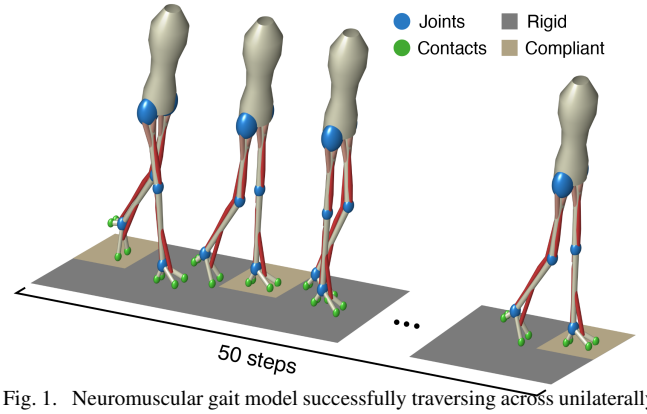

Fig. 1. Neuromuscular gait model successfully traversing across unilaterally soft ground. Sand patches are simply used to illustrate the difference in stiffness between the ground and the left and right feet. While only a brief portion is shown, the model remained upright and walked in a straight line for 50 seconds in this condition. On average this amounted to 50 steps with each leg. Joints and contact points can be seen in blue and green, respectively. All 11 muscles can be seen on each leg, with the four that are analyzed in this paper in a darker shade of red.

human data collected in a similar environment. We show that the proposed model can explain quite accurately the human data at both a kinematic and muscle activation level in this unique walking environment. This proper understanding and accurate modeling of human gait in this environment will directly allow for better control of bipedal robots in comparable terrains. Additionally, since this asymmetrically soft environment has been suggested to be useful for the rehabilitation of paretic gait, the ability to accurately describe with this model the human response at both a kinematic and neuromuscular level could allow for advances in model-informed, patient-specific rehabilitation strategies in the future.

II. Methods

A. Overview

In this study, we built upon the neuromuscular gait model developed by Song and Geyer [18], enabling it to describe the complex condition of walking on unilateral low-stiffness ground. The data produced by this model is compared to human data collected in the same environment, consequently validating the model in this particular scenario.

B. Model Description

The three-dimensional neuromuscular human gait model, developed by Song and Geyer, is used in this study [18] (see Fig. 1). This model is comprised of 7 total segments: the trunk, as well as left and right thighs, shanks, and feet. These segments take on inertial and geometric properties that are estimated from human data. Also, these segments are manipulated with 22 Hill-type muscle-tendon units, 11 for each leg [19]. All of the segments are connected by revolute joints. These joints are 2 degrees of freedom (DoF) at the hips and 1 DoF at the knees and ankles. This model interacts with the environment through 4 contact points on each foot. These contact points represent the medial ball, lateral ball, medial heel, and lateral heel of each foot [18].

This gait model is controlled through two main layers: the supraspinal layer and the spinal layer. First, the supraspinal layer makes big-picture decisions, such as calculating desired foot placement at heel strike, setting a desired target trunk angle to be maintained throughout an entire walking trial, and setting a desired maximum height the foot should be lifted off the ground during swing phase to avoid toe drag. Additionally, the supraspinal layer decides when a leg should transition from stance phase to swing phase, ending the double support phase of gait. The spinal layer then takes the information from the supraspinal layer and executes 10 reflex modules, 5 for the stance phase and 5 for swing phase. These 10 modules are (from heel strike to heel strike): realize leg at heel strike, prevent knee over-extension, balance the trunk, compensate for swing leg torques, plantarflex the ankle during push-off, swing the hip forward to begin the swing phase, flex the knee to avoid toe drag, hold the knee in this flexed state, stop the leg from swinging once the target foot placement location is approaching, and hold the leg over this location until heel strike occurs [18]. Evaluating these 10 reflex modules results in the stimulation of the 22 muscle-tendon units which then activate to generate motion in the model.

At a more general level, the model is calibrated for different environments using 82 control parameters. These parameters act as gains that modulate how the above modules and processes are completed. These parameters will be discussed in more detail below as they were used to extend and calibrate the model to the two environments in this study (rigid and unilaterally compliant). For more details on the model, see previous works [18, 20, 21].

C. Model Calibration and Initialization

For this study, the neuromuscular gait model is calibrated for and walks in two different environments: rigid and unilaterally compliant. For the rigid condition, the stiffness of the interaction between both feet and the ground is 1 MN/m, which represents walking on a hard surface such as concrete. For the unilaterally compliant condition, the stiffness of the interaction between the model's left foot and the ground is 45 kN/m, which is considered to be similar to walking on a soft yoga mat. This was chosen to best fit the Variable Stiffness Treadmill (VST), the main tool used for the human experiment, discussed below. The interaction with the right foot and the ground for this condition remains rigid (stiffness of 1 MN/m). For both conditions, the model was given a desired forward walking speed of 120 cm/s.

D. Model Optimization

The model is programmed in MATLAB (Mathworks, Inc.) using Simulink SimMechanics and the *ode15s* solver function. Optimization of the 82 control parameters described above was completed using the Covariance Matrix Adaptation Evolution Strategy (CMA-ES) method [22]. A population size of 64 (the number of trials in each generation) was evaluated over 100 generations, resulting in a total of about 6400 trials per optimization run. Each trial

was 20 seconds long unless the model fell over, in which case the trial was stopped early. A standard deviation of 0.05 to 0.4 was used to describe the search window for each parameter. Additionally, when appropriate, upper and lower bounds were used for individual parameters to prevent meaningless solutions from being found. With an 82-dimensional parameter space, initial conditions are extremely important, as falling into undesirable local minima may easily occur. Because of this, initial guesses for each parameter were chosen very carefully based on experience and the related literature. If the optimizer found a working solution for the desired environment, that "best solution" was often used as the initial condition for follow-up optimization runs.

For the condition of rigid ground for both legs, 82 control parameters were used. Seven of these parameters are used to adjust foot placement control, 4 are for transitions from stance to swing and swing to stance phases, 40 are for stance reflex modules, and 31 are for swing reflex modules. For the unilaterally soft condition, 83 control parameters were used. An additional parameter was added, allowing the model to control left and right step lengths more independently. This was done in response to the human data, which will be discussed below. For more information on these control parameters, see previous works and the accompanying model MATLAB code [18, 23].

The cost function used for this optimizer is comprised of three tiers. Once a certain condition is met, the cost function switches to a lower tier resulting in a lower cost function value (J). More specifically, the cost function initially attempts to keep the model upright for the entire 20-second trial. If this is achieved, the cost function then aims to have the model converge to steady walking in the final six steps of the trial. If this is accomplished, the final tier of the cost function attempts to match the desired velocity, minimize energy usage, and match step length trends from human data for the last four steps with each leg. This cost function is very similar to the cost function found in Song & Geyer's study, with a few modifications and additions [18]. The cost can be seen explicitly and is explained in more detail below:

$$J = \begin{cases} 2c_0 - x_f & \text{, if fall} \\ c_0 + d_S & \text{, if non-steady walking} \\ a\sum_{i=1}^{n} |\mathbf{v_{tgt}} - \mathbf{v}_i| + C_E + 10c_0 s_e & \text{, if steady walking} \end{cases} \tag{1}$$

where $|\mathbf{b}|$ is the Euclidean norm of $\mathbf{b}$, $c_0 = 1000$ is a constant parameter, x_f is the distance walked before falling, d_S is a numeric representation of steadiness in the last six steps of the trial (discussed more below), $a = 0.0025$ is a constant parameter, i is the time step counter, n is the total number of time steps, $\mathbf{v_{tgt}}$ is the two-dimensional desired velocity of $[1.2, 0]^T$ (in the horizontal plane), $\mathbf{v}_i$ is the instantaneous center of mass velocity at each time step i, C_E is the energy expended (discussed more below), and s_e is the step length error (discussed more below).

Steadiness in the final six steps is calculated using the summed differences of the three-dimensional Cartesian positions of the hip and knee joints relative to the ankle at heel strike. For example, on the third to last left heel strike, the position of the left hip is found with respect to the left ankle. This is repeated for the last two left steps as well, then the average of these three positions is found. The hip coordinates for each of the last three steps is then subtracted from the average, the absolute value is taken, and then all three are summed together and the Euclidean norm is taken. This process is also duplicated for the left knee, right hip, and right knee. The results of all four processes are then summed to obtain a single value that estimates steadiness. This can be seen explicitly below:

$$d_S = d_L + d_R \tag{2}$$

where

$$\begin{aligned} d_L &= \textstyle\sum_{j=1}^{3} \left|\mathbf{x}_{L,j}^{h/a} - \bar{\mathbf{x}}_L^{h/a}\right| + \sum_{j=1}^{3} \left|\mathbf{x}_{L,j}^{k/a} - \bar{\mathbf{x}}_L^{k/a}\right| \\ d_R &= \textstyle\sum_{j=1}^{3} \left|\mathbf{x}_{R,j}^{h/a} - \bar{\mathbf{x}}_R^{h/a}\right| + \sum_{j=1}^{3} \left|\mathbf{x}_{R,j}^{k/a} - \bar{\mathbf{x}}_R^{k/a}\right| \end{aligned} \tag{3}$$

where j represents the step counter that takes into account the last three steps with each leg, $\mathbf{x}^{h/a}$ is the three-dimensional Cartesian coordinates of the hip with respect to the ankle, $\mathbf{x}^{k/a}$ is the three-dimensional Cartesian coordinates of the knee with respect to the ankle, $\bar{\mathbf{x}}$ is the average three-dimensional Cartesian coordinates of the hip and knee with respect to the ankle, and L and R denote the left and right legs respectively. If d_S is below a certain value, the model's walking is denoted as "steady," and the third tier of the cost function is evaluated.

Energetic cost is calculated by first finding the area under the activation vs. time curve for each muscle. This value is then multiplied by the maximum force each muscle is capable of producing. All muscles are summed together and this value is divided by the mass of the model times the total distance the model traveled. This can be seen below:

$$C_E = \frac{\sum_{k=1}^{22} F_{max,k} \int_0^{t_f} A_k \, dt}{m \, x_f} \tag{4}$$

where k represents each of the 22 muscles in the model, $F_{max,k}$ is the max force of each muscle, t_f is the total time of the trial, A_k is the muscle activation (from 0 to 1), m is the mass of the model, and x_f is the total distance traveled.

The step length deviations l_e and r_e for the left and right legs respectively are simply the squared difference between desired step length and actual step length for the last four steps with each leg. Desired step lengths for left and right legs are equal for rigid ground and different for unilaterally soft terrain (to mimic human data, see below). Those step length deviations are then added to obtain the total step length error:

$$s_e = l_e + r_e \tag{5}$$

where

$$\begin{aligned} l_e &= \textstyle\sum_{m=1}^{4} (L_{SL} - c_L)^2 \\ r_e &= \textstyle\sum_{m=1}^{4} (R_{SL} - c_R)^2 \end{aligned} \tag{6}$$

Fig. 2. Subject walking on the VST equipped with electromyographic (EMG) sensors and reflective markers for motion capture. The body weight harness can be partially seen around the subject's torso.

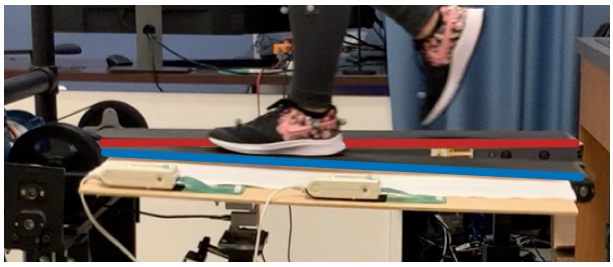

Fig. 3. VST simulating a unilateral low stiffness environment. The left belt (blue) is set to 45 kN/m and the right belt (red) is set to rigid (1 MN/m). As the left leg steps on the compliant belt, the belt deflects vertically due to its reduced stiffness.

where m represents the step counter for the final four steps with each leg, L_{SL} is the left step length of the model, R_{SL} is the right step length of the model, and c_L, c_R are the desired step lengths respectively. For rigid, they were set to $c_L = c_R = 0.62$, while for unilaterally compliant, they were set to $c_L = 0.63$ and $c_R = 0.68$. These values were selected based on trends seen in the human data discussed below.

E. Human Experiment

The human experiment was performed on the Variable Stiffness Treadmill (VST), which is our unique, split-belt robotic treadmill (see Fig. 2) [13]. The VST has the capability of reducing the vertical stiffness of the left belt, while the right belt remains rigid (see Fig. 3). This can simulate interesting environments, such as walking with one foot on sand, and the other on concrete. For more information on the VST, see our previous works [24, 25].

Eight healthy subjects participated in this study [13]. Mirroring the experiment with the model, this experiment had two main sections: walking on rigid and walking on unilaterally compliant surfaces. In the rigid phase, subjects walked for 100 gait cycles with both sides of the treadmill set to rigid (i.e. normal treadmill walking). This rigid stiffness is estimated to be 1 MN/m on the VST. During the unilaterally compliant section of the experiment, subjects walked for 400 gait cycles with the left side of the treadmill set to 45 kN/m and the right side of the treadmill still set to rigid. The unilaterally compliant phase is much longer, as subjects take longer to acclimate themselves in this unusual environment. The goal of this study is to observe the steady-state gait that is produced in each of these environments. In other words, we are not interested in the transient effects that may occur as the subjects adapt to walking on each surface. Therefore, this study will only focus on the steady-state gait that is achieved at the end of each of the two sections. Particularly, only the last 30 gait cycles of each phase will be considered. Note that the value of 30 gait cycles was chosen to isolate data that has converged to a steady state while maintaining enough data points to draw conclusions.

During this experiment, subjects were equipped with 22 reflective markers used for motion capture. Additionally, subjects wore four electromyographic (EMG) sensors on each leg to measure the muscle activity of their tibialis anterior (TA), gastrocnemius (GA), vastus medialis (VA), and biceps femoris (BF). While each subject wore a support harness when walking on the VST, this harness was not offloading any of the subject's weight. The harness was only for safety precautions and no subject was forced to rely on it during any trials (see Fig. 2). Each subject selected their own walking speed from the options of 80, 85, and 90 cm/s which is deemed comfortable for walking on the VST. Note that these walking speeds are slower than the walking speed of the model. This is due to the model being taller than all human subjects. More details about the experiment and the data pre-processing can be found in our previous study [13].

III. Results

The goal of this study is to show that the proposed neuromuscular (NMS) gait model can accurately simulate human walking in a unilaterally soft environment. This will be validated at a functional, kinematic, and muscular level in order to prove that the model is an adequate representation of human motor control during walking in this environment.

One important objective of the model is reaching steady-state walking as human subjects did. Although the model was optimized for a 20-second trial, when tasked with a 50-second trial, the model succeeded in converging to a steady state solution, proving its ability to continue past the bounds it was optimized for (see Fig. 4). This is seen as the step lengths remain steady for the 30 steps plotted in Fig. 4.

Regarding model validation, it must be noted that what is important when validating the responses of the model against the human experimental data is not the absolute values, but the trends found when comparing data from unilaterally compliant and rigid environments. This is analyzed in the next subsections. Additionally, for all results, the unilaterally compliant environment will be compared to the rigid environment. In other words, stating an "increased activation" for a particular muscle is describing a higher activation for that muscle in the unilaterally compliant scenario than that in the rigid scenario.

A. Functional Outcomes

At the simplest level, the model simulates human walking accurately. First, this complex 3D gait model is able to stay upright and achieve consistent, steady locomotion.

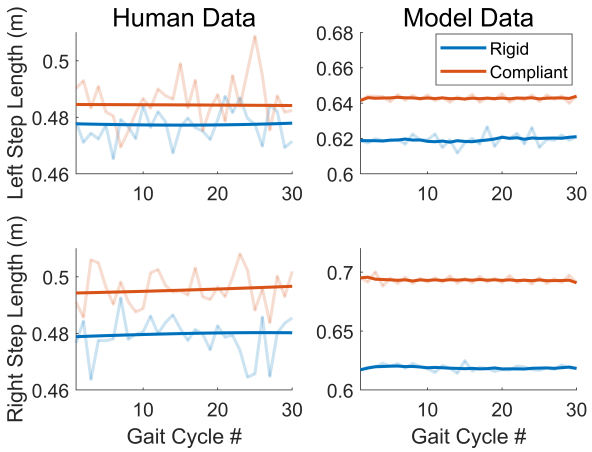

Fig. 4. Step length data for human subjects (left) and the NMS model (right) in both rigid and left side compliant environments. Step length was measured as the distance between ankles at left or right heel strike. Human data is the last 30 steps averaged between all eight subjects. Model data is simply the last 30 steps for a single trial for each environment. Unfiltered data is seen for both the model and the human in the lighter lines. Darker lines represent smoothed data using 2^{nd} degree polynomial local regression.

Additionally, as seen in Fig. 4, the model displays similar step length trends in the unilaterally compliant scenario as compared to the rigid scenario. While step length was part of the cost function, it is still notable that the model successfully traverses this challenging environment with the prescribed "human" trend of asymmetric increased step length. Comparing the human and model numerically, the human data shows a 1.97% increase in left step length and a 3.55% increase in right step length, while the model shows a 3.79% increase in left step length and a 12.02% increase in the right step length. Again, while numerically these increases are not equivalent, the correct trend can be seen in the model when compared to human data: an increase in left step length, and a larger increase in right step length.

B. Kinematics

Regarding kinematics, the model simulates the human data well, following most of the trends seen. Note that only the hip and knee flexion-extension angles throughout the gait cycle will be examined. The ankle joint will not be discussed since the model's ankle kinematics have a poor correlation to human data on rigid ground. This is one of the major shortcomings of this model [18]. Also, note that we are defining a gait cycle from left heel strike to the following left heel strike. All data is normalized in this fashion.

As shown in Fig. 5, for the left hip, little to no separation is seen in the human data between the rigid and compliant cases. This pattern is emulated in the model fairly well. For the right hip, however, delayed flexion can be seen in the human data during right swing. The model shows a very similar response. This delayed flexion contributes toward the large increase in step length on the right side. Waiting longer in the gait cycle to swing the hip forward allows the distance between ankles to increase prior to heel strike.

Similarly, as shown in Fig. 5, the left knee in the human data displays both increased flexion in early left stance and delayed and increased flexion in left swing. Both of these features are clearly simulated in the model. For the right knee, the model matches the delayed and slight increase in flexion during right swing as seen in the human data. Increased flexion during swing can also help contribute to producing a larger step length. Increased knee flexion reduces the moment of inertia of the leg, allowing it to be swung farther forward with reduced effort [26]. In summary, the model was able to predict changes in kinematics when comparing the rigid and unilaterally compliant conditions, which agree with changes observed in human data.

C. Muscle Activity

For understanding human motor control in the studied environments, it is important that the model generated muscle activations that resemble those seen in human data. It was seen that the model mimics human muscle activity trends and timing well in this unique environment (see Fig. 5). While a few of the muscles observed do not match entirely, this was expected. A similar level of correspondence can be seen in previous works for other simpler environments [18, 21]. Additionally, multiple muscle activation signals saturate to a maximum activation level. This will be further addressed in future studies.

While the model's activation timing appears to be accurate in the left TA, the model does not match the magnitude trends seen in the human data very well. This appears to be due to an overall lack of activation variance in the rigid trial for the model. For the right TA, an increased activation can be seen soon after right toe-off and after right heel strike in the human data. This can also be seen in the model. While the model doesn't show a decreased activation during mid-swing of the right leg, it does show a decreased activation soon after the initial left heel strike, as seen in the human data. The left GA of the model successfully simulates the major feature seen in this muscle in the human data: an increased and delayed peak during late stance of the right leg. Additionally, the model correctly shows the increased activity in late left swing (90% to 100%). This increased activation prior to left toe-off most likely causes a greater push-off force and contributes to the increased step length seen in the left leg. The right GA of the model shows increased activation before right toe-off, as is also seen in the human data. The model does not, however, show a higher peak after left toe-off. This is due to the muscle on the model being saturated at 100%. Again, this increased activation prior to right toe-off likely helps produce an increased step length. Similarly, the left VA of the model does not show higher activation in early left stance. Again, the model data becomes saturated at that point. The model does however increase the muscle activity earlier in the gait cycle for the left VA, mimicking the human data. The same trend is seen with the right VA. Due to saturation, the model cannot display a higher peak around 50% to 60%, but it does show an earlier increase, therefore increasing the overall work done by the right VA during early right stance, just as the human data shows. This increased activation seen in the left and right VA could be a response to an increased step length. With the heel strike occurring farther forward,

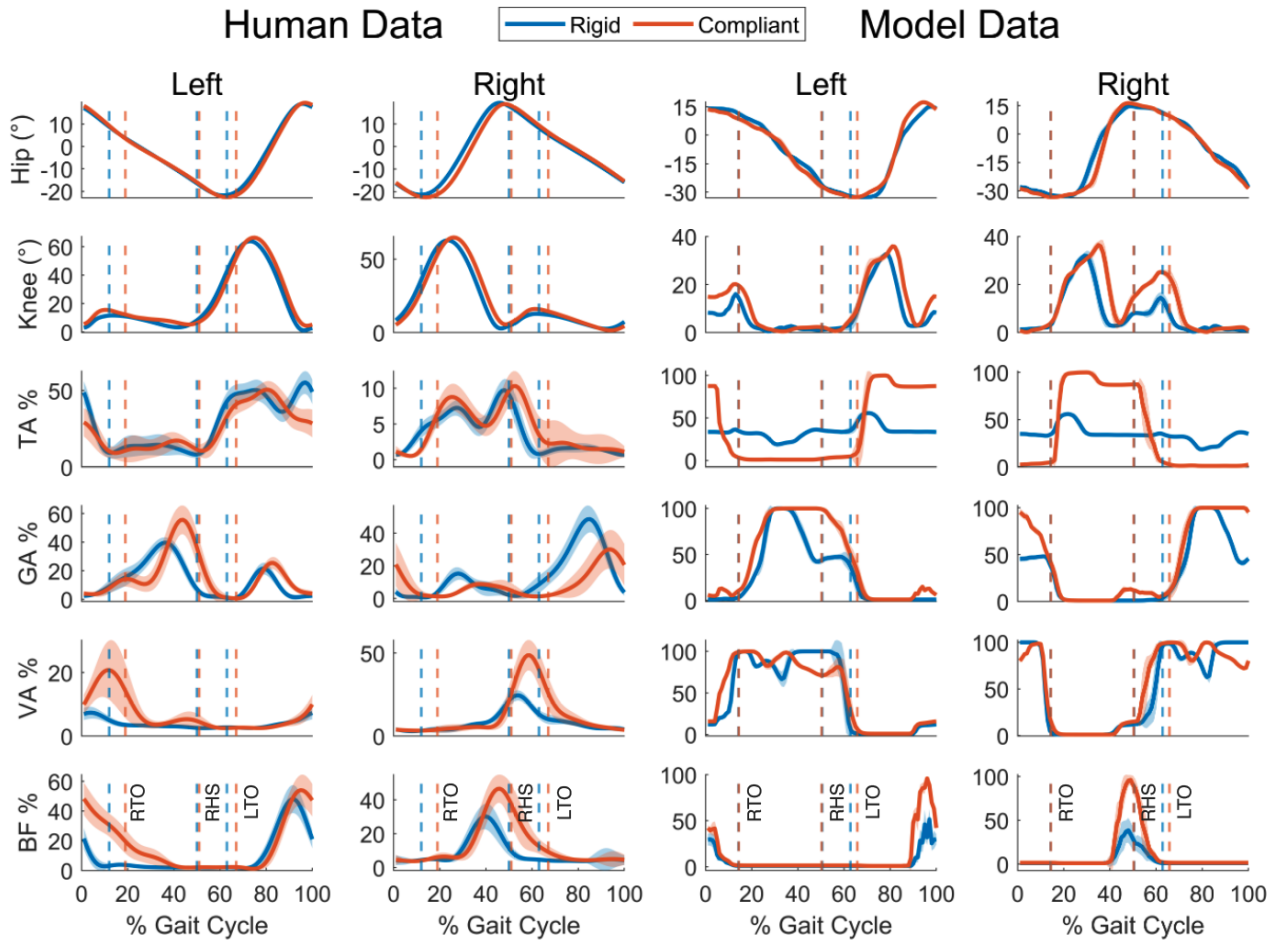

Fig. 5. Kinematic and muscle activity data from human subjects (left) and the proposed NMS model (right) in two environments: rigid (blue) and unilaterally compliant (orange). Hip and knee kinematic data are shown in the first two rows. Muscle activity data is shown in the last four rows, and it is displayed in percent activation, normalized with respect to a maximum activation value. For the human data, the last 30 gait cycles of the rigid and unilaterally compliant phases for a representative subject were averaged and plotted. For the model data, the last 30 steps were averaged for a single trial in each environment. Standard deviations can be seen in shaded areas. Note that standard deviation areas are in every plot, even though some are too small to clearly see. Gait cycles are sectioned from left heel strike (LHS) to left heel strike, so this occurs at 0 and 100%. In this order, right toe-off (RTO), right heel strike (RHS), and left toe-off (LTO) are shown on average for each environment for the human and model data as vertical dashed lines.

the knee is more susceptible to buckling, and the VA may activate more to keep the knee stable. For the left BF, very similar trends are seen in the model and human data during late left swing and early left stance. Both the model and human data show an increased activation and nearly zero activation for the rest of the gait cycle. Likewise, for the right BF, the same results are seen. The model successfully mimics the major feature of the human data: an increased activation around right heel strike. Again both the human and the model show nearly zero activation otherwise. In summary, the proposed model succeeds in capturing not only the profiles of human muscle activations but also the changes in these activations observed when comparing the unilaterally compliant environment to the rigid environment.

IV. Conclusions

This study presents a neuromuscular gait model that has been adapted to accurately simulate human locomotion on unilaterally compliant terrain. Through the comparison with experimental human data, this model is validated, as both human and model data show many of the same trends when walking on unilaterally soft ground as compared to rigid. Therefore, the adapted model can describe functional, kinematic, and muscle activation changes seen in similar experiments with humans. This is an important contribution to modeling and characterizing human gait motor control in complex environments, which can lead to advances in two main fields. First, we believe this model could be quite useful for stroke rehabilitation, as unilateral stiffness perturbations have shown promise to correct common issues found in hemiplegic gait. Being able to accurately model the human response to those perturbations could lead to patient-specific treatments. The next step in developing this model for further use in rehabilitation is to check the model's accuracy in different environments. Second, the knowledge gained from this model could lead to the development of bio-inspired controllers for bipedal robots, giving them the ability to traverse through dynamic and complaint terrains.

REFERENCES

[1] D. R. J. Bassett, H. R. Wyatt, H. Thompson, J. C. Peters, and J. O. Hill, "Pedometer-Measured Physical Activity and Health Behaviors in U.S. Adults," *Medicine & Science in Sports & Exercise*, vol. 42, no. 10, pp. 1819–1825, Oct. 2010.

[2] Welton JM, Decker M, Adam J, and Zone-Smith L, "Research for practice. How far do nurses walk?" *MEDSURG Nursing*, vol. 15, no. 4, pp. 213–216, Aug. 2006.

[3] S. E. H. Davies and S. N. Mackinnon, "The energetics of walking on sand and grass at various speeds," *Ergonomics*, vol. 49, no. 7, pp. 651–660, Jun. 2006.

[4] M. E. L. van den Berg, C. J. Barr, J. V. McLoughlin, and M. Crotty, "Effect of walking on sand on gait kinematics in individuals with multiple sclerosis," *Multiple Sclerosis and Related Disorders*, vol. 16, pp. 15–21, Aug. 2017.

[5] Y. Zheng, H. Wang, S. Li, Y. Liu, D. Orin, K. Sohn, Y. Jun, and P. Oh, "Humanoid robots walking on grass, sands and rocks," in *2013 IEEE Conference on Technologies for Practical Robot Applications (TePRA)*, Apr. 2013, pp. 1–6.

[6] A. S. P. Sousa and J. M. R. S. Tavares, "Interlimb Coordination During Step-to-Step Transition and Gait Performance," *Journal of Motor Behavior*, vol. 47, no. 6, pp. 563–574, Nov. 2015.

[7] J. Skidmore, A. Barkan, and P. Artemiadis, "Investigation of contralateral leg response to unilateral stiffness perturbations using a novel device," in *IEEE International Conference on Intelligent Robots and Systems*. Institute of Electrical and Electronics Engineers Inc., Oct. 2014, pp. 2081–2086.

[8] J. Skidmore and P. Artemiadis, "Unilateral Floor Stiffness Perturbations Systematically Evoke Contralateral Leg Muscle Responses: A New Approach to Robot-Assisted Gait Therapy," *IEEE Transactions on Neural Systems and Rehabilitation Engineering*, vol. 24, no. 4, pp. 467–474, Apr. 2016.

[9] J. Skidmore and P. Artemiadis, "Unilateral walking surface stiffness perturbations evoke brain responses: Toward bilaterally informed robot-assisted gait rehabilitation," in *Proceedings - IEEE International Conference on Robotics and Automation*, vol. 2016-June. IEEE, May 2016, pp. 3698–3703.

[10] V. Chambers and P. Artemiadis, "A Model-based Analysis of Supraspinal Mechanisms of Inter-leg Coordination in Human Gait: Toward Model-informed Robot-assisted Rehabilitation," *IEEE Transactions on Neural Systems and Rehabilitation Engineering*, vol. 29, pp. 1–1, 2021.

[11] P. W. Duncan, R. Zorowitz, B. Bates, J. Y. Choi, J. J. Glasberg, G. D. Graham, R. C. Katz, K. Lamberty, and D. Reker, "Management of Adult Stroke Rehabilitation Care," *Stroke*, vol. 36, no. 9, Sep. 2005.

[12] S. Li, G. E. Francisco, and P. Zhou, "Post-stroke hemiplegic gait: New perspective and insights," *Frontiers in Physiology*, vol. 9, no. AUG, p. 1021, Aug. 2018.

[13] V. Chambers and P. Artemiadis, "Repeated Robot-assisted Unilateral Stiffness Perturbations Result in Significant Aftereffects Relevant to Post-Stroke Gait Rehabilitation," in *IEEE International Conference on Robotics and Automation (ICRA)*. IEEE, 2022.

[14] C. Karakasis, I. Poulakakis, and P. Artemiadis, "Robust Dynamic Walking for a 3D Dual-SLIP Model under One-Step Unilateral Stiffness Perturbations: Towards Bipedal Locomotion over Compliant Terrain," in *2022 30th Mediterranean Conference on Control and Automation (MED)*. Vouliagmeni, Greece: IEEE, Jun. 2022, pp. 969–975.

[15] M. Wang, M. Wonsick, X. Long, and T. Padr, "In-situ Terrain Classification and Estimation for NASA's Humanoid Robot Valkyrie," in *2020 IEEE/ASME International Conference on Advanced Intelligent Mechatronics (AIM)*, Jul. 2020, pp. 765–770.

[16] G. Mesesan, J. Englsberger, G. Garofalo, C. Ott, and A. Albu-Schäffer, "Dynamic Walking on Compliant and Uneven Terrain using DCM and Passivity-based Whole-body Control," in *2019 IEEE-RAS 19th International Conference on Humanoid Robots (Humanoids)*, Oct. 2019, pp. 25–32.

[17] D. Yao, L. Yang, X. Xiao, and M. Zhou, "Velocity-Based Gait Planning for Underactuated Bipedal Robot on Uneven and Compliant Terrain," *IEEE Transactions on Industrial Electronics*, vol. 69, no. 11, pp. 11 414–11 424, Nov. 2022.

[18] S. Song and H. Geyer, "A neural circuitry that emphasizes spinal feedback generates diverse behaviours of human locomotion," *Journal of Physiology*, vol. 593, no. 16, pp. 3493–3511, Aug. 2015.

[19] H. Geyer and H. Herr, "A Muscle-reflex model that encodes principles of legged mechanics produces human walking dynamics and muscle activities," *IEEE Transactions on Neural Systems and Rehabilitation Engineering*, vol. 18, no. 3, pp. 263–273, 2010.

[20] S. Song and H. Geyer, "Generalization of a muscle-reflex control model to 3D walking," in *Proceedings of the Annual International Conference of the IEEE Engineering in Medicine and Biology Society, EMBS*, vol. 2013. Annu Int Conf IEEE Eng Med Biol Soc, 2013, pp. 7463–7466.

[21] S. Song and H. Geyer, "Evaluation of a neuromechanical walking control model using disturbance experiments," *Frontiers in Computational Neuroscience*, vol. 11, p. 15, 2017.

[22] N. Hansen, "The CMA Evolution Strategy: A Comparing Review," in *Towards an New Evolutionary Computation*, 2006, pp. 75–102.

[23] S. Song, "Neuro-muscular-skeletal simulation model of human locomotion," http://seungmoon.com/nmsModel/nmsModel.html, 2022.

[24] A. Barkan, J. Skidmore, and P. Artemiadis, "Variable Stiffness Treadmill (VST): A novel tool for the investigation of gait," in *Proceedings - IEEE International Conference on Robotics and Automation*. Institute of Electrical and Electronics Engineers Inc., Sep. 2014, pp. 2838–2843.

[25] J. Skidmore, A. Barkan, and P. Artemiadis, "Variable Stiffness Treadmill (VST): System Development, Characterization, and Preliminary Experiments," *IEEE/ASME Transactions on Mechatronics*, vol. 20, no. 4, pp. 1717–1724, Aug. 2015.

[26] L. C. Smith and B. Hanley, "Comparisons between swing phase characteristics of race walkers and distance runners," *International Journal of Exercise Science*, vol. 6, no. 4, pp. 269–277 (9), Oct. 2013.